



## Two-element acoustic array gives insight into ice-ocean interactions in Hornsund Fjord, Spitsbergen

Oskar GŁOWACKI <sup>1\*</sup>, Grant B. DEANE <sup>2</sup>, Mateusz MOSKALIK <sup>1</sup>,  
Jarosław TĘGOWSKI <sup>3</sup> and Philippe BLONDEL <sup>4</sup>

<sup>1</sup> *Instytut Geofizyki, Polska Akademia Nauk – Centrum Studiów Polarnych,  
ul. Księcia Janusza 64, 01-452 Warszawa, Poland  
<oglowacki@igf.edu.pl> <mmosk@igf.edu.pl>*

<sup>2</sup> *Scripps Institution of Oceanography, University of California in San Diego,  
9500 Gilman Drive, La Jolla, CA 92093, USA <gdeane@ucsd.edu>*

<sup>3</sup> *Wydział Oceanografii i Geografii, Uniwersytet Gdański,  
Al. M. Piłsudskiego 46, 81-378 Gdynia, Poland <j.tegowski@ug.edu.pl>*

<sup>4</sup> *Department of Physics, University of Bath,  
Claverton Down, Bath, BA2 7AY, UK <pyspb@bath.ac.uk>*

\* *corresponding author*

**Abstract:** Glacierized fjords are dynamic regions, with variable oceanographic conditions and complex ice-ocean interactions, which are still poorly understood. Recent studies have shown that passive underwater acoustics offers new promising tools in this branch of polar research. Here, we present results from two field campaigns, conducted in summer 2013 and spring 2014. Several recordings with a bespoke two-hydrophone acoustic buoy were made in different parts of Hornsund Fjord, Spitsbergen in the vicinity of tidewater glaciers to study the directionality of underwater ambient noise. Representative segments of the data are used to illustrate the analyses, and determine the directions of sound sources by using the time differences of arrivals between two horizontally aligned, broadband hydrophones. The results reveal that low frequency noise (< 3 kHz) is radiated mostly from the ice cliffs, while high-frequency (> 3 kHz) noise directionality strongly depends on the distribution of floating glacial ice throughout the fjord. Changing rates of iceberg production as seen for example in field photographs and logs are, in turn, most likely linked to signal amplitudes for relevant directions. These findings demonstrate the potential offered by passive acoustics to study the dynamics of individual tidewater glaciers.

Key words: Tidewater glaciers, ice melting, passive acoustics, Spitsbergen, Hornsund.

### Introduction

Interactions between the ocean and ice bodies are among the most dynamic, often unpredictable processes seen in the Arctic. Marine-terminating glaciers are losing

their mass primarily as a result of calving and submarine melting, thereby providing significant quantities of cold fresh water to the glacial bays and fjords (*e.g.* Jacob *et al.* 2012; Gardner *et al.* 2013). This mass loss raises eustatic sea level and modifies local water circulation patterns (*e.g.* Motyka *et al.* 2003; Straneo *et al.* 2011).

Much effort has therefore been put in the last decades into investigating these issues. Various methods are commonly used, including for example seismic surveys and satellite imaging (see *e.g.* Bartholomaeus *et al.* 2012; Błaszczuk *et al.* 2013). They are however often limited by their temporal and spatial resolutions. In the case of commonly available satellite imagery, most small-scale (< 100-m) processes (*e.g.* local glacier ablation) cannot be detected or quantified, and repeatability (*i.e.* the time between successive images) is too low to detect and understand dynamic processes sometimes occurring within seconds (*e.g.* calving episodes). Local marine measurements, such as temperature, salinity and currents, are also often used to get insight into ice-ocean interactions, *e.g.* how much freshwater is contributed by melting ice, or how currents affect drifting ice distribution (*e.g.* Motyka *et al.* 2013; Straneo *et al.* 2011). They are, however, usually limited in space to the profiles taken, and in time to the actual surveys. The only exceptions are more costly oceanographic moorings with numerous conductivity-temperature-depth (CTD) sensors, Acoustic Doppler Current Profilers (ADCPs) or other devices. Moreover, field measurements are also hampered by the limitations associated with the harsh polar conditions, which should ideally limit the need for continuous human involvement.

Passive underwater acoustics provides new possibilities to measure some of these variations and ice-ocean interaction in general, offering inexpensive options for continuous or long-term monitoring over large areas and with high spatial and temporal resolution (*e.g.* Pettit *et al.* 2012; Głowacki and Moskalik 2014). Acoustic waves propagate well in water, carrying quantitative information over long distances (Medwin 2005). Cold War applications, in the early 1960s, focused on Arctic sound propagation and sea ice. The first published spectral analyses of Arctic noise (Urlick 1971) focused on the noise of melting ice blocks, indicating that escaping, tiny air bubbles could produce very loud sounds. These findings were confirmed in the field and in laboratory experiments using real growlers (*e.g.* Tęgowski *et al.* 2011, 2012; Blondel *et al.* 2013; Lee *et al.* 2014; Pettit *et al.* 2015). Other very loud sound sources are also present. Sound pressure levels for Hornsund Fjord, Spitsbergen often exceed 100 dB re 1  $\mu$ Pa, even in calm weather (Tęgowski *et al.* 2011). Similarly, annual averages of 120 dB re 1  $\mu$ Pa were measured in Icy Bay, Alaska, with a peak between 1 and 3 kHz (Pettit *et al.* 2015). The acoustic signatures of ice detachments from tidewater glaciers in Svalbard and Alaska (Pettit 2012; Tęgowski *et al.* 2012; Głowacki *et al.* 2015) show that calving events produce ambient noise mainly below a few kilohertz, as a result of pre-calving activity, disintegrations, generation of mini-tsunamis, ice-water impacts and ice-ice interactions. Using passive acoustics it was possible to detect individual ice detachments, and for the first time to distinguish different types of calving (Głowacki *et al.* 2015).

This diversity of sound sources requires that they be unambiguously separated, in time and in space. Deane *et al.* (2014) measured underwater acoustics in the foreground of the Hans Glacier in the Hornsund Fjord, Spitsbergen with a two-element, bespoke Directional Acoustic Buoy (DAB). They showed that different, spatially diverse sources generate underwater ambient noise in distinct frequency bands.

Here we present measurements of the ambient noise directionality, carried out in various places in the same fjord, close to several marine-terminating glaciers. Building on the study by Deane *et al.* (2014), the main goal was to find out whether it is possible to distinguish between underwater sounds coming from the ice cliffs and those originating elsewhere in the fjord. An affirmative answer would open new avenues for the application of hydrophone arrays to quantitative measurements of dynamic processes at the ice-ocean boundaries.

## Study area

Hornsund Fjord is located in the southern part of Spitsbergen, the biggest island of the Svalbard Archipelago. The fjord is currently ~35 km long, for an area greater than 300 km<sup>2</sup>. There are five glacierized bays in Hornsund (Fig. 1), clearly distinguished by the strongly developed coastline: Hansbugta, Vestre and Austre Burgerbukta, Samarinvågen and Brepollen. Several valley-type tidewater glaciers flow into the fjord, creating the topography of this region. Cumulatively, their calving cliffs were found to be almost 35 km long in 2010. According to recent studies (Błaszczuk *et al.* 2013), the retreat of tidewater glaciers in Hornsund is much faster than in other regions in Svalbard, with average rates of ~70 m a<sup>-1</sup>. Along their marine margins, they have lost ~142 km<sup>2</sup> between 1899 and 2010. Among the contributing factors, relatively warm marine climate and significant exposure to inflows of warm Atlantic water are indicated as the most crucial (Błaszczuk *et al.* 2013).

## Methods

Acoustic recordings, each lasting from 30 minutes to 1 hour, were taken in different regions of Hornsund in August 2013 and April 2014. Locations of these eight measurement sites are shown in Fig. 1, indicating that attention was focused on the vicinities of various tidewater glaciers. Measurement sites are named according to the date (YYMMDD) and order number (/n), when several recordings were taken the same day (*e.g.* 130822/2 is the 2<sup>nd</sup> measurement taken on 22 August 2013).

The DAB was deployed from a rubber boat, with its two broadband hydrophones (International Transducer Corporation 6050C) spaced apart by  $D = 0.43$  m on a horizontal axis, a magnetic compass and a GPS sensor (see more details in Deane *et al.* 2014). During the deployment, the horizontal axis of the receivers was

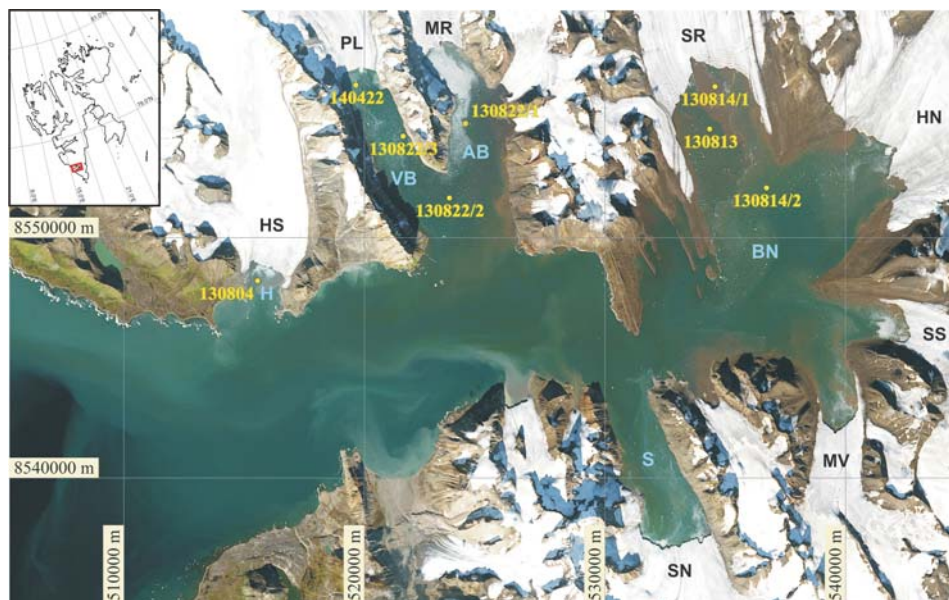


Fig. 1. Locations of the study sites inside Hornsund Fjord, Spitsbergen. The largest tidewater glaciers are marked with abbreviations as follows: HS – Hans, PL – Paierl, MR – Mühlbacher, SN – Samarin, SR – Stor, HN – Horn, SS – Svalis, MV – Mendeleev. Similarly, five glacierized bays can be identified as: H – Hansbugta, VB – Vestre Burgerbugta, AB – Austre Burgerbugta, BN – Brepollen, S – Samarinvågen. Landsat-8 image collected on August 24, 2013, courtesy of the U.S. Geological Survey, Department of the Interior. Color figures are available online in electronic version at <http://www.degruyter.com/view/j/popore>.

submerged to a depth of approximately 1 m. A portable digital audio recorder was used to record both hydrophone channels synchronously and with 48 kHz sampling frequency. Each session started with a 1-min recording of white noise, generated with a Gold Line PN2W noise generator providing a continuous signal at a set spectral level, for repeated calibration of the measurement system. Selecting periods with almost windless weather made it possible to reduce the contribution of background noise from unwanted sources, such as breaking waves and surf, and conduct the recordings in accordance with established best practice (Robinson *et al.* 2014). Additionally, paper logs and high-resolution photographs of all especially loud events, like ice detachments or collision between the boat and floating ice, were supplemented with details of the ice conditions around the sites.

Earlier studies showed that lower frequencies corresponded to calving events (Tęgowski *et al.* 2012; Głowacki *et al.* 2015), pre-calving activity and probably also to freshwater outflows (Pettit 2012). They also showed that ambient noise above 2.5 kHz is normally distributed (Tęgowski *et al.* 2012). Calving events generate ambient noise predominantly at frequencies below 200 Hz, but which can also be pronounced in the frequency band 1–3 kHz (Głowacki *et al.* 2015, fig. 1d–i). Measurements were therefore divided in two frequency bands, 20 Hz –

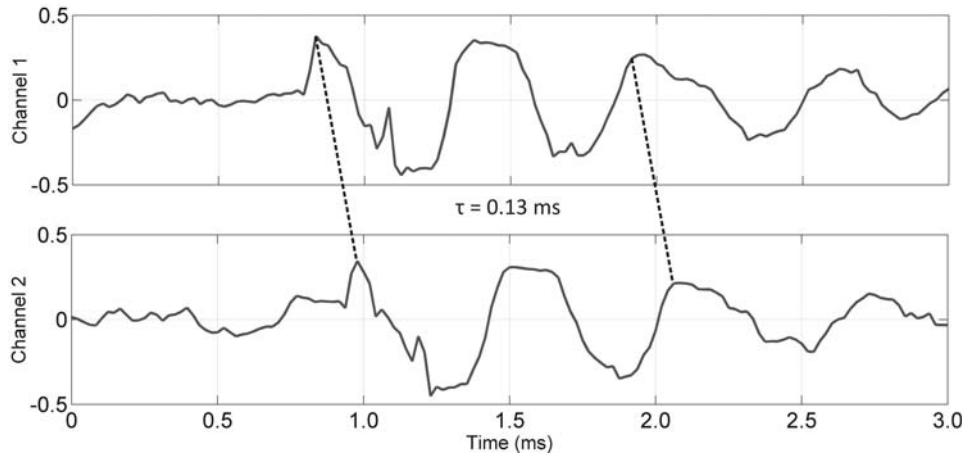


Fig. 2. Example of two short acoustic signals received concurrently by a pair of hydrophones. Time delay depends directly on the angle of arrival.

3 kHz and 3 kHz – 20 kHz, using digital band-pass filters during post-processing of the signals. Higher-frequency sounds are attenuated rapidly with increasing distance to the source. According to the modified Thorpe equation, attenuation of noise with a frequency of 10 kHz reaches around 6 dB at 5 kilometers and is almost an order of magnitude higher than for 2 kHz (see equation 1.47 in Jensen *et al.* 2011). This increases the importance of nearby sources like ice growlers, which melt in the water, and of bubble events, which can be pronounced even at frequencies higher than 10 kHz (see *e.g.* fig. 4d in Pettit *et al.* 2015).

Time differences between arrivals at each hydrophone were derived from the normalized cross-correlation between short segments of noise. These segments were 1.36 and 0.34 s long, respectively, for lower and higher frequency bands (Deane *et al.* 2014). An example of two time-shifted segments is shown in Fig. 2. The argument corresponding to the maximum value of the cross-correlation function gives information about the time delay  $\tau_d$ . Using the sound speed  $c$ , calculated to be 1460  $\text{ms}^{-1}$  for the prevailing hydrographic conditions (see CTD profiles in Moskalik *et al.* 2014; unpublished data), the angle of arrival relative to the axis of the acoustic array (Fig. 3) is given by:

$$\theta = \arccos\left(\frac{\tau_d c}{D}\right) \quad (1)$$

Unambiguous estimation of arrival angles yielding the same time delay (*e.g.* arrivals from  $60^\circ$  and  $300^\circ$ ) is not possible, as they both correspond to the same maximum value of  $\tau_d$ . To re-

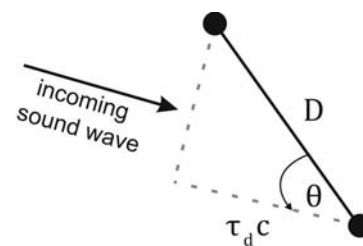


Fig. 3. Geometry between incoming sound wave and 2-element acoustic array with a length  $D$ . Knowing the speed of sound  $c$  and time difference of arrival, the angle of arrival can be readily calculated (see Eq. 1).

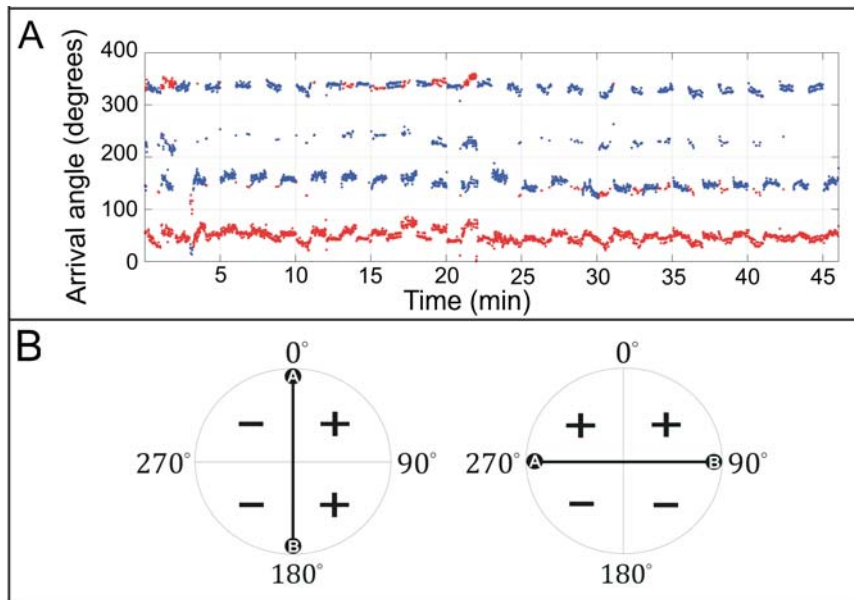


Fig. 4. Arrival angle versus time in the frequency range 20 Hz – 3 kHz for the site 130822/2, located in Burgerbugta (A), together with simple scheme illustrating array rotations performed every minute during each deployment (B). Angles (relative to North: 0°) were calculated taking into account the DAB orientation. Red dots correspond to pluses and blue to minuses, which means respectively arrivals from the right and left side of the array (colors visible in the online version). If the sources are stable, as in this case, real arrivals from the same direction remain relatively constant after the rotation. For example, the source located at ~50° was still active, while the other one at ~150° was particularly loud between 29 and 36 minute of the recording.

duce this ambiguity, the DAB was rotated by 90° every 1 minute during the recordings (see Fig. 4). This procedure assumes relative stability of the sound sources and, therefore, works better for stationary ice cliffs than *e.g.* for floating ice blocks. The ability to determine the arrival angles can be also improved by measuring the noise field for a longer period of time, tens of minutes in this case.

The resolving power of a 2-hydrophone array and the accompanying theory are extensively discussed in Deane 1999. Of relevance here is the higher resolution for higher frequencies and for sound waves coming closer to parallel to the axis of the acoustic array.

## Results of the acoustic measurements

**Site 130804 (summer).** — Recordings were taken in Hansbugta, about a kilometer south from the face of Hans Glacier, with a relatively small amount of floating ice blocks close to the boat. Directionality of the ambient noise field in this particular location was similar for both analyzed frequency ranges, as shown on the

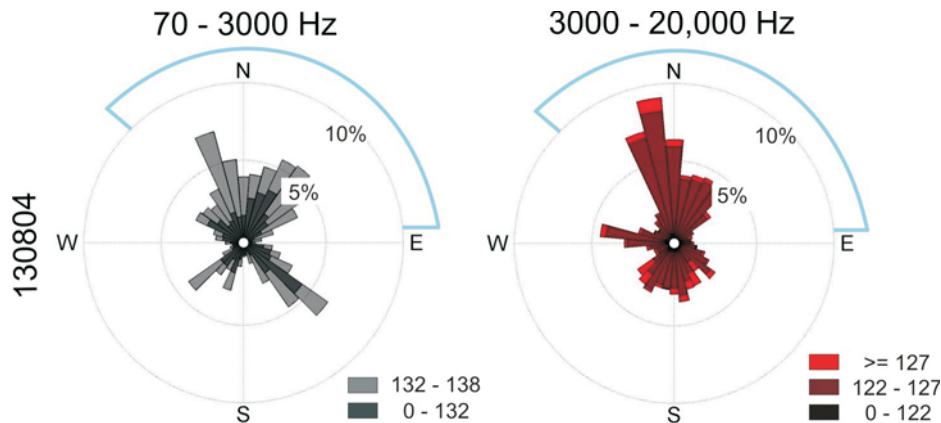


Fig. 5. Rose plots of the ambient noise directionality for site 130804, located close to the Hans Glacier in Hansbugta. Color scales illustrate the proportion of arrivals with specific intensity, coming from each direction. Numerical values are the result of cross-correlation, normalized by the number of samples taken for calculations, and correspond to dB re  $1 \mu\text{Pa}^2$ . Blue bars point to the glacier fronts.

rose plots (Fig. 5). Most arrivals point toward the ice cliff. However, some portion also came from the opposite direction.

**Sites 130822/1–3 (summer).** — Ambient noise was recorded (Fig. 6) at three different locations in Burgerbugta:  $\sim 5$  km south from the Mühlbacher Glacier (Fig. 1; 130822/1), in the central part of the glacial bay (Fig. 1; 130822/2), and  $\sim 5$  km southeast from the Paierl Glacier (Fig. 1; 130822/3). In the latter case, the boat drifted very close to the shoreline, which could significantly affect acoustic measurements through the effects of sediment absorption and horizontal refraction. For that reason, results from this location are not discussed further, but are presented anyway to serve as a guide for future deployments. Rose plots for the first site clearly show that low frequency noise came mostly from the calving front, while high frequency sounds seem to be generated by different, spatially scattered sources. Blocks of ice of different sizes, from a few centimeters to several meters in diameter, covered a substantial part of the sea surface during these measurements. There were also two other smaller glaciers to the east and northeast. The noise directionality at site 130822/2 was relatively similar for both sets of frequencies and illustrates that most arrivals are from the northeastern and northwestern parts of Burgerbugta. Additional low frequency arrivals from the southeast point to glaciers further away.

**Site 140422 (spring).** — This recording (Fig. 7), made in April, is a good example of directivity patterns for lower water temperature and relatively less active tidewater glaciers in the fjord. While low frequency ambient noise still comes mostly from the glacier calving front, high frequency arrivals point primarily to the west and south. Sound levels are also significantly smaller than during summer.

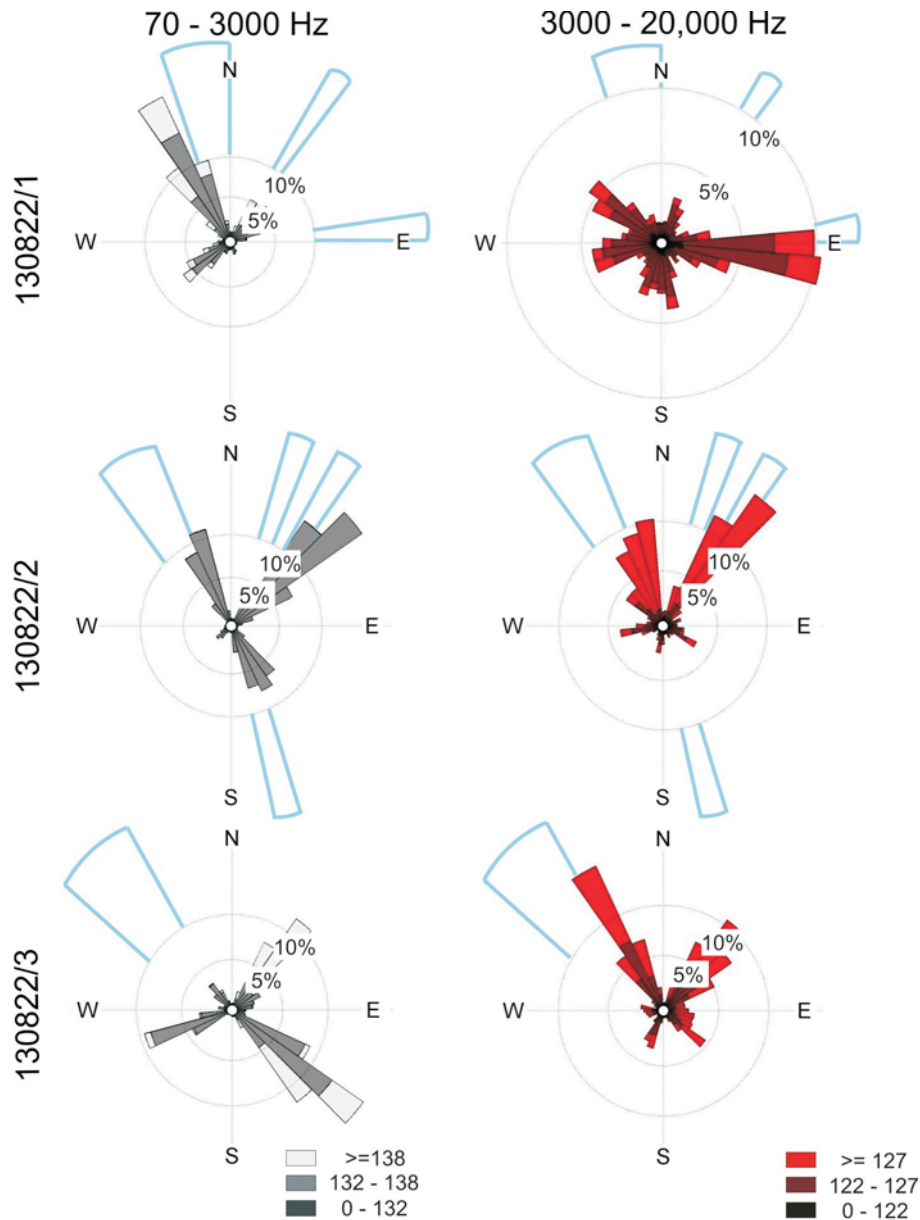


Fig. 6. Rose plots of the ambient noise directionality for sites 130822/1–3, located in Burgerbugta. Blue bars point to the glacier fronts.

**Sites 130813 and 130814/1–2 (summer).** — There were three measurement sites in Brepollen, located at the end of the Hornsund Fjord: ~1 and 3 km south from the Stor Glacier (Fig. 1; 130814/1 and 130813, respectively) as well as in the center part of the glacial bay (Fig. 1; 130814/2). In general (Fig. 8), noise directionality patterns are similar as at Burgerbugta. For example, the low-fre-

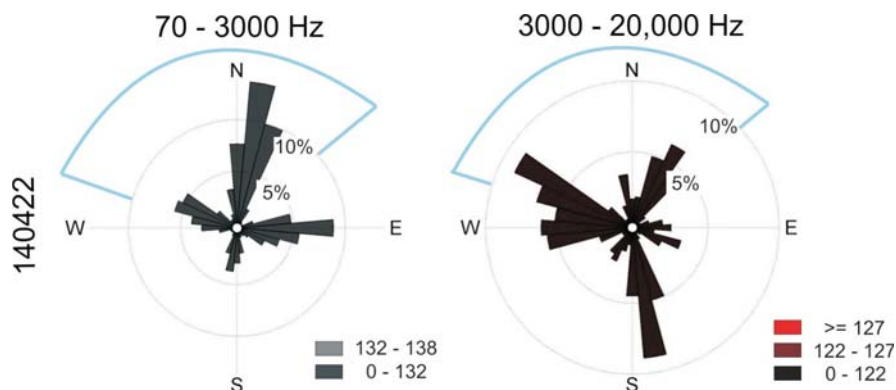


Fig. 7. Rose plots of the ambient noise directionality for site 140422, located close to the Paiarl Glacier in Burgerbugta. Blue bars point to the glacier fronts.

quency rose plot for site 130814/2 shows arrivals pointing to all glaciers in a direct line of sight. Louder levels are received from the northeast and southeast than from the northwest. However, there are some differences. High frequency sounds recorded at the site 130813 were coming practically from all directions. Moreover, at this station, low-frequency signals were arriving not only from the ice cliff at the north, but also from the shoreline. According to the field log, there were a lot of floating blocks of ice around the boat at this location, but Stor Glacier later calved much less frequently than neighboring Horn Glacier. This situation persisted until the end of the measurements. It should also be emphasized that low- and high-frequency sounds at site 130814/1, close to the glacier front, seem to originate from two specific sections of the calving cliff. Both the most intensive and most frequent arrivals point toward the center part of the wall.

## Discussion and conclusions

As shown in the previous section, underwater sounds in the frequency band 20 Hz – 3 kHz come mainly from the ice cliffs. This new finding is even more clearly visible in the central parts of the glacial bays (see Fig. 9). The sound levels of low-frequency arrivals from these directions seem to correspond well to the calving intensity of individual tidewater glaciers, recorded in the field notes (site 130814/2 in Figs 8, 9B) and possibly even match the activity of specific portions (site 130814/1 in Fig. 8). Taken together, these results suggest that underwater acoustic arrays, deployed in Arctic fjords for long periods, can offer a unique opportunity to track glacier dynamics in an autonomous and continuous way.

Conversely, the directionality of high-frequency underwater sounds is strongly connected with the amount and spatial distribution of blocks of glacial ice floating around the fjords. This is confirmed by the differences observed between periods of significant ice mass compared with relatively ice-free conditions, especially when

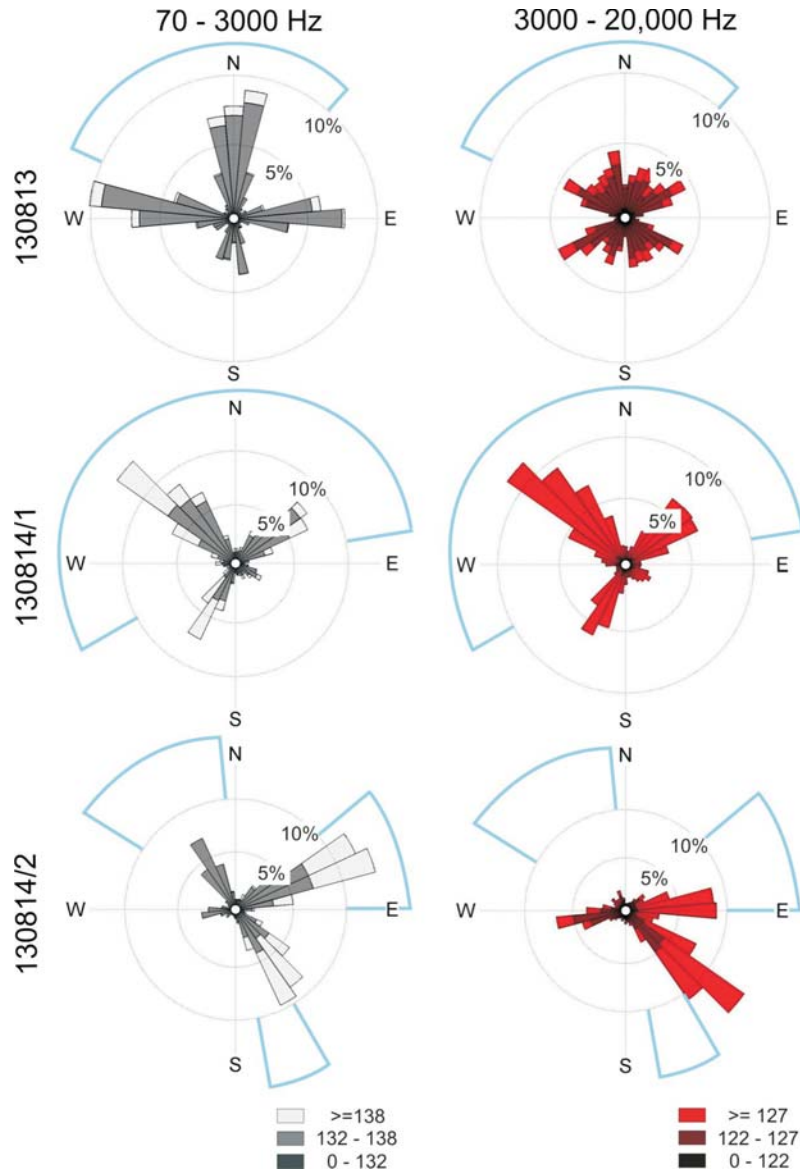


Fig. 8. Rose plots of the ambient noise directionality for sites 130813 and 130814/1–2, located in Brepollen. Blue bars point to the glacier fronts.

the boat drifted close to the ice walls, when high- and low-frequency signals were coming practically from the same directions (see rose plots for sites 130804 and 130814/1 in Figs 5, 8). This also quantifies the importance of melting at the ice cliff, when comparing with other sources of noise in fjords containing glaciers. These measurements underline the importance of monitoring drifting ice concentrations while acoustic monitoring techniques are in their development phase.

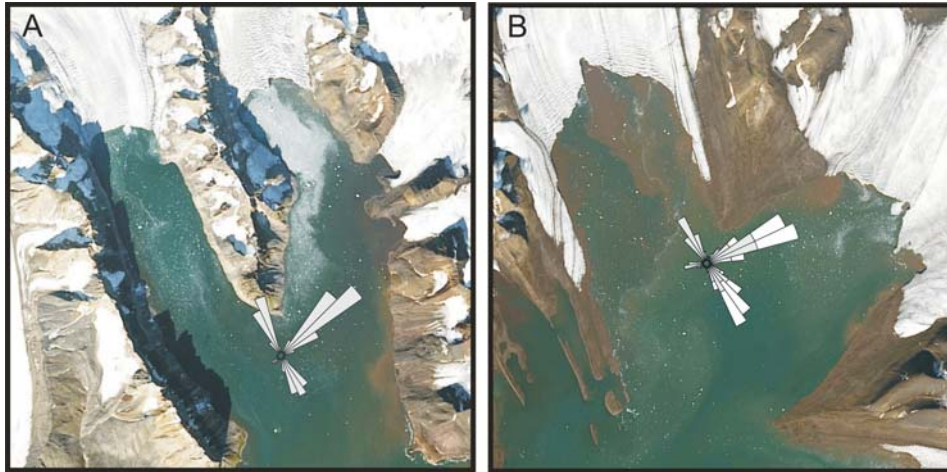


Fig. 9. Rose plots of the low-frequency ambient noise directionality for sites 130822/2 (A) and 130814/2 (B), superimposed on the corresponding parts of the satellite image from Fig. 1. Except that medium gray was replaced with light gray, the color scale is similar as for Figs 5–8.

The use of two hydrophones has enabled the detection of spatially distinct sources, despite an inherent ambiguity in the measurement of arrival angle (corrected here with regular re-orientation of the DAB frame). This did not prove a problem for the relatively short examples shown here, and the latest field tests (summer 2014) investigated the advantages of using a third hydrophone compared to its additional constraints (more difficult deployment and exact positioning, higher data rates and slightly more complex processing).

At all frequencies, propagation affects ambient noise directionality (Jensen *et al.* 2011). Cold freshwater supplied by tidewater glaciers changes sound speed, which depends on temperature and salinity (Głowacki *et al.* 2013). CTD and ADCP profiles taken in Hansbugta indicate that fresh water outflows tend to create narrow zones of low sound speed with varying horizontal and vertical structure (Moskalik *et al.* 2014). Acoustic energy can therefore be channeled along these water layers (acting as waveguides), often localized just below the sea surface (Głowacki *et al.* 2013). Moreover, seabed topography (*e.g.* the presence of a sill) and other obstacles (*e.g.* promontories, islands) also affect sound propagation. Acoustic measurements show excellent promise as a tool for long-term monitoring of ice-ocean interactions at scales varying from very local (tens of meters) to fjord-scale (kilometers and more).

**Acknowledgements.** — The authors were supported by the Polish National Science Center grant 2011/03/B/ST10/04275, Research Council of Norway *Arctic Field Grant* RIS ID: 6133 and USA Office of Naval Research, Ocean Acoustics Division grant N00014-14-1-0213. This work was partially supported within statutory activities No 3841/E-41/S/2015 of the Ministry of Science and Higher Education of Poland. We also appreciate the valuable help from Joanna

Ćwiąkała and Piotr Dolnicki during field measurements. The rose plots were prepared using a modified version of wind\_rose.m by P. Remo, <http://www.mathworks.com/matlabcentral/fileexchange/17748-wind-rose>. We would like to acknowledge the reviews contributed by Prof. Zygmunt Klusek and the detailed and very helpful comments of Prof. Erin Pettit.

## References

- BARTHOLOMAUS T.C., LARSEN C.F., O'NEEL S. and WEST M.E. 2012. Calving seismicity from ice-berg-sea surface interactions. *Journal of Geophysical Research* 117: F04029.
- BŁASZCZYK M., JANIA J.A. and KOLONDRĄ L. 2013. Fluctuations of tidewater glaciers in Hornsund Fjord (Southern Svalbard) since the beginning of the 20th century. *Polish Polar Research* 34 (4): 327–352.
- BLONDEL P., TĘGOWSKI J. and DEANE G.B. 2013. Laboratory analyses of transient ice cracking in growlers. *Proceedings of 1st International Conference and Exhibition on Underwater Acoustics*. Corfu, Greece: 1253–1260.
- DEANE G.B. 1999. Acoustic hot spots and breaking wave noise in the surf zone. *Journal of the Acoustical Society of America* 105 (6): 3151–3167.
- DEANE G.B., GŁOWACKI O., TĘGOWSKI J., MOSKALIK M. and BLONDEL P. 2014. Directionality of the ambient noise field in an Arctic, glacial bay. *Journal of the Acoustical Society of America* 136 (5): EL350.
- GARDNER A.S., MOHOLDT G., COGLEY J.G., WOUTERS B., ARENDT A.A., WAHR J., BERTHIER E., HOCK R., PFEFFER W.T., KASER G., LIGTENBERG S.R.M., BOLCH T., SHARP M.J., HAGEN J.O., VAN DEN BROEKE M.R. and PAUL F. 2013. A reconciled estimate of glacier contributions to sea level rise: 2003–2009. *Science* 340: 852–857.
- GŁOWACKI O. and MOSKALIK M. 2014. Application of passive hydroacoustics in the studies of sea-ice, icebergs and glaciers: Issues, approaches and future needs. In: R. Bialik, M. Majdański and M. Moskalik (eds) *Geoplanet: Earth and Planetary Sciences 2014: Achievements, History and Challenges in Geophysics*, Springer-Verlag, Berlin: 271–295.
- GŁOWACKI O., MOSKALIK M. and PROMIŃSKA A. 2013. *Simulation of the sound propagation in an Arctic fjord: general patterns and variability*. Poster presented at: Arctic Science Summit Week, Session: Marine Processes and Variability, April 17–19, Kraków, Poland, URL: <http://www.eposters.net/poster/simulation-of-the-sound-propagation-in-an-arctic-fjord-general-patterns-and-variability>.
- GŁOWACKI O., DEANE G.B., MOSKALIK M., BLONDEL P., TĘGOWSKI J. and BŁASZCZYK M. 2015. Underwater acoustic signatures of glacier calving. *Geophysical Research Letters* 42: 804–812.
- JACOB T., WAHR J., PFEFFER W.T. and SWENSON S. 2012. Recent contributions of glaciers and ice caps to sea level rise. *Nature* 482: 514–518.
- JENSEN F.B., KUPERMAN W.A., PORTER M.B. and SCHMIDT H. 2011. *Computational Ocean Acoustics*, 2nd Edition. Springer, New York: 794 pp.
- LEE K.M., WILSON P.S. and PETTIT E.C. 2014. Underwater sound radiated by bubbles released by melting glacier ice. *Proceedings of Meetings on Acoustics* 20: 070004.
- MEDWIN H. 2005. *Sounds in the Sea: From Ocean Acoustics to Acoustical Oceanography*. Cambridge University Press, Cambridge: 664 pp.
- MOSKALIK M., GŁOWACKI O., PROMIŃSKA A. and ĆWIAKAŁA J. 2014. The effect of Hansbreen tide-water glacier on the hydrography of Isbjørnhamna (Hornsund, Svalbard). Poster presented at: 35th Polar Symposium – Diversity and state of polar ecosystems, June 4–7, Wrocław, Poland, URL: <http://www.eposters.net/poster/the-effect-of-hansbreen-tidewater-glacier-on-the-hydrography-of-isbjrnhamna-hornsund-svalbard>.

- MOTYKA R.J., HUNTER L., ECHELMAYER K.A. and CONNOR C. 2003. Submarine melting at the terminus of a temperate tidewater glacier, LeConte Glacier, Alaska, USA. *Annals of Glaciology* 36: 57–65.
- MOTYKA R.J., DRYER W. P., AMUNDSON J., TRUFFER M. and FAHNESTOCK M. 2013. Rapid submarine melting driven by subglacial discharge, LeConte Glacier, Alaska. *Geophysical Research Letters* 40: 5153–5158.
- PETTIT E.C. 2012. Passive underwater acoustic evolution of a calving event. *Annals of Glaciology* 53: 113–122.
- PETTIT E.C., NYSTUEN J.A. and O'NEEL S. 2012. Listening to glaciers: Passive hydroacoustics near marine-terminating glaciers. *Oceanography* 25: 104–105.
- PETTIT E.C., LEE K.M., BRANN J.P., NYSTUEN J.A., WILSON P.S. and O'NEEL S. 2015. Unusually loud ambient noise in tidewater glacier fjords: A signal of ice melt. *Geophysical Research Letters* 42: 2309–2316.
- ROBINSON S.P., LEPPER P.A. and HAZELWOOD R.A. 2014. *Good practice guide for underwater noise measurement*. National Measurement Office, Marine Scotland, The Crown Estate, NPL Good Practice Guide No. 133: 95 pp.
- STRANEO F., CURRY R.G., SUTHERLAND D.A., HAMILTON G.S., CENEDESE C., VÅGE K. and STEARNS L. A. 2011. Impact of fjord dynamics and glacial runoff on the circulation near Helheim Glacier. *Nature Geoscience* 4: 322–327.
- TEGOWSKI J., DEANE G.B., LISIMENKA A. and BLONDEL P. 2011. Detecting and analyzing underwater ambient noise of glaciers on Svalbard as indicator of dynamic processes in the Arctic. *Proceedings of the 4th UAM Conference*, Kos, Greece: 1149–1154.
- TEGOWSKI J., DEANE G.B., LISIMENKA A. and BLONDEL P. 2012. Spectral and statistical analyses of ambient noise in Spitsbergen Fjords and identification of glacier calving events. *Proceedings of the 11th European Conference on Underwater Acoustics*, Edinburgh, Scotland: 1667–1672.
- Urlick R. J. 1971. The noise of melting icebergs. *Journal of the Acoustical Society of America* 50: 337.

Received 1 July 2015

Accepted 18 November 2015